Peakbagging in the open cluster NGC 6819: Opening a treasure chest or Pandora's box?

Handberg, R.; Miglio, A.; Brogaard, K.; Bossini, D.; Elsworth, Y.~P.

[Link to publication on Research at Birmingham portal](#)

Peakbagging in the open cluster NGC 6819
– Opening a treasure chest or Pandora's box?

R. Handberg[1,2,⋆]**, A. Miglio**[2]**, K. Brogaard**[1]**, D. Bossini**[2]**,** and **Y. P. Elsworth**[2]

[1] Stellar Astrophysics Centre (SAC), Department of Physics and Astronomy, Aarhus University, Denmark.
[2] School of Physics and Astronomy, University of Birmingham, UK.

Here we report on an extensive peakbagging effort on the evolved red giant stars of the open cluster NGC 6819. This consists of around 50 stars spanning all the way up the red giant branch (RGB) and down to and including the red clump (RC). These stars represent a unique sample, because of their common distance, metallicity and age. By employing sophisticated pre-processing of the time series and Markov Chain Monte Carlo (MCMC) techniques we have extracted individual frequencies, heights and line widths for hundreds of individual oscillation modes in the sample of stars. We show that average asteroseismic parameters derived from these can be used to distinguish the stellar evolutionary state between RGB and RC stars, without having to measure the often difficult dipole modes. Furthermore, we show how the fitting of some of these dipole modes can improve the detectability of acoustic glitches arising from the Helium II ionization zone and how this can potentially be used to constrain the Helium content in the cluster. We also discuss some of the difficulties facing similar studies in the future, where it seems that detailed studies of star clusters are facing some difficult times ahead.

1 Introduction

Asteroseismology, the study of acoustic oscillations in stars, is an immensely powerful tool for accurately determining properties of stars such as their masses, radii and ages. Traditionally stellar clusters, because of their members common chemical composition, distance and age, provide unique samples of stars ideal for detailed studies of stellar evolution. Therefore, performing detailed asteroseismology on a large sample of stars in a stellar cluster will provide strong constraints on stellar models, by combining the constraints from "classical" cluster studies with asteroseismology. Here we report on such a study performed using high-quality data from the *Kepler* mission (Borucki et al. 2010). A full publication of the work which reported on here is currently in prep. (Handberg et al.).

Asteroseismilogy of solar-like and red giant stars centres around the measurement of *p*-mode oscillations in the stellar material through the minute changes in stellar brightness caused by the oscillations. The *p*-mode oscillation frequencies of a solar-like star is approximatively described by:

$$\nu_{n\ell} \approx \Delta\nu(n + \ell/2 + \epsilon) - \delta\nu_{0\ell}\,, \tag{1}$$

where $\Delta\nu$ is the large frequency separation, n and ℓ are the radial orders and angular degrees respectively, ϵ is a phase

shift introduced by surface effects and $\delta\nu_{0\ell}$ is the small frequency separation. Modes therefore form a regular pattern centred around the characteristic frequency of maximum power, ν_{max}. Once the stars evolve into red giants and ascent the red giant branch (RGB) and finally reaches the red clump (RC), additional oscillation modes can be measured as a result of interactions with *g*-modes in the dense core (see e.g. Mosser et al. 2012). These modes are separated (nearly) equally in period with the characteristic separation ΔP. Determinations of global asteroseismic parameters, like $\Delta\nu$, ν_{max} and $\delta\nu_{0\ell}$, can be used to obtain global stellar properties through grid-based modelling and scaling relations (see e.g. Chaplin et al. 2014; Quirion et al. 2010; Silva Aguirre et al. 2015). However, if the individual oscillation frequencies can be determined, much more detailed information about the stellar structure and evolution can be obtained.

For *Kepler* Red Giant stars, detailed "*peak-bagging*", meaning the extraction of individual oscillation modes and all their characteristics, has only been performed for a handful of stars. The discipline has proven itself extensively for main-sequence and sub-giant stars, but has not been applied to a large extent to evolved Red Giants. This has mainly been due to complications introduced by the many mixed dipole modes.

⋆ Corresponding author: rasmush@phys.au.dk

2 Data preparation

The open cluster NGC 6819 (age ~ 2.5 Gyr, [Fe/H] ~ 0.07) was observed throughout the *Kepler* mission in long cadence mode (LC; $\delta t = 29.8$ min). Unfortunately NGC 6819 falls on one of the parts of the *Kepler* field-of-view which was affected by the failure of one of the CCD modules approximately one year into the mission. This means that, due to the unstable roll of the spacecraft about its pointing axis, the time series has a three months gap every year.

The calibrated pixel-level data for NGC 6819 was processed using the prescriptions described in Handberg & Lund (2014), but because of the crowded field of the cluster the normal procedure of enlarging the apertures to allow more stellar flux through the aperture (see Handberg & Lund 2014, and references therein) in some cases caused elevated noise or contamination. Therefore all targets were manually checked and the mask producing the best light curves in terms of noise-characteristics were used for the final analysis.

Finally the weighted power density spectrum of the flux time series was calculated for all targets using statistical weights on each point to minimize the white noise contribution.

3 Global asteroseismic parameters

The first analysis done to the power density spectra is to fit the background arising primarily from the surface granulation. Since no physical model exists for the shape of the background, we perform this fit using all of the following empirical formulations which are commonly used (Harvey 1985; Kallinger et al. 2012; Karoff 2008):

$$N(\nu) = \eta(\nu) \cdot \sum_{k=1}^{2} \frac{4\sigma_k^2 \tau_k}{1 + (2\pi\nu\tau_k)^2} + K \qquad (2)$$

$$N(\nu) = \eta(\nu) \cdot \sum_{k=1}^{2} \frac{4\sigma_k^2 \tau_k}{1 + (2\pi\nu\tau_k)^4} + K \qquad (3)$$

$$N(\nu) = \eta(\nu) \cdot \sum_{k=1}^{2} \frac{4\sigma_k^2 \tau_k}{1 + (2\pi\nu\tau_k)^2 + (2\pi\nu\tau_k)^4} + K \qquad (4)$$

$$N(\nu) = \eta(\nu) \cdot \sum_{k=1}^{2} \frac{4\sigma_k^2 \tau_k}{(1 + (2\pi\nu\tau_k)^2)^2} + K \qquad (5)$$

where σ_k and τ_k is the amplitudes and timescales of each component, K is the white noise level. The frequency dependent factor $\eta(\nu) \equiv \mathrm{sinc}^2(\Delta T_{\mathrm{int}} \cdot \nu)$ is the attenuation arising from gathering the data over a time-span, ΔT_{int} (the exposure time), which in case of *Kepler* long cadence data is 1765.5 s. Additionally a Gaussian envelope accounting for the oscillation power is added. The highest point in this envelope is defined as ν_{max}, and the resulting combined model power spectrum is defined as follows:

$$P(\nu) = N(\nu) + \eta(\nu) \, a_{\mathrm{env}} \exp\left[\frac{-(\nu - \nu_{\mathrm{max}})^2}{2\sigma_{\mathrm{env}}^2}\right] \qquad (6)$$

where a_{env} and σ_{env} denote the height and width of the envelope respectively. This model is fitted to the full power spectrum and the large frequency separation, $\Delta\nu$, is then estimated from calculating the power spectrum of the power spectrum in the frequency range $\nu_{\mathrm{max}} \pm 2\sigma_{\mathrm{env}}$. In each case, the background fit and large separation calculation are iterated three times to yield consistent result. Finally the background with the lowest Bayesian Information Criterion (BIC) is selected as the final background. Once the optimal shape of the background has been chosen, the fitted parameters are passed as first guesses to a Markov chain Monte Carlo method (Handberg & Campante 2011) which yields the final values of the parameters and corresponding error estimates.

4 Peakbagging

From a simple look at the power spectra of the oscillating cluster stars, it becomes apparent that they empirically fall into three overall categories, examples of which are shown in Fig. 1. The low luminosity RGB stars are characterised by clear radial and quadrupole ($\ell = 0, 2$) modes with clear "dipole forest" (see e.g. Bedding et al. 2011; Mosser et al. 2012) and the dipole modes clearly separated from each other. As we move below $\nu_{\mathrm{max}} \sim 60\,\mu$Hz the dipole forest merge into single unresolved peaks, in fact very reminiscent of the pattern known from main-sequence solar-like stars. Because of the high quality of the *Kepler* data it was possible to go to the next stage in the analysis and perform detailed *peakbagging*, fitting the individual oscillation modes and extracting individual frequencies, heights, mode lifetimes, rotational splittings and inclination angle. The peakbagging was performed using the prescriptions of Handberg & Campante (2011), but using slightly different strategies for fitting the dipole modes in each of the three empirical groups. In all cases we used single Lorentzian functions to describe the radial and quadrupole modes. We are therefore ignoring any rotational splitting or mixed modes in the quadrupole modes. This also means that we are in fact measuring a weighed average of any mixed quadrupole modes. For the high luminosity RGB (clean dipole) stars, we fitted the dipole modes in a similar manner. The frequencies we extract are therefore weighted averages of any unresolved mixed dipole modes. For low RGB stars where the dipole modes are distinguishable from each other we included the individual mixed dipole modes in the fit, including a free rotational splitting for each mode, where it was possible. In the cases where this was not possible, we simply excluded the frequency-regions in the power spectrum containing power from the dipole modes from the likelihood calculation and only fitted the radial and quadrupole modes. The latter was also the case for the red clump stars, whose dipole frequency structure is very complicated and therefore very difficult to robustly peakbag.

In summary, the end result is that we for all stars were able to fit the radial and (average) quadrupole modes, plus
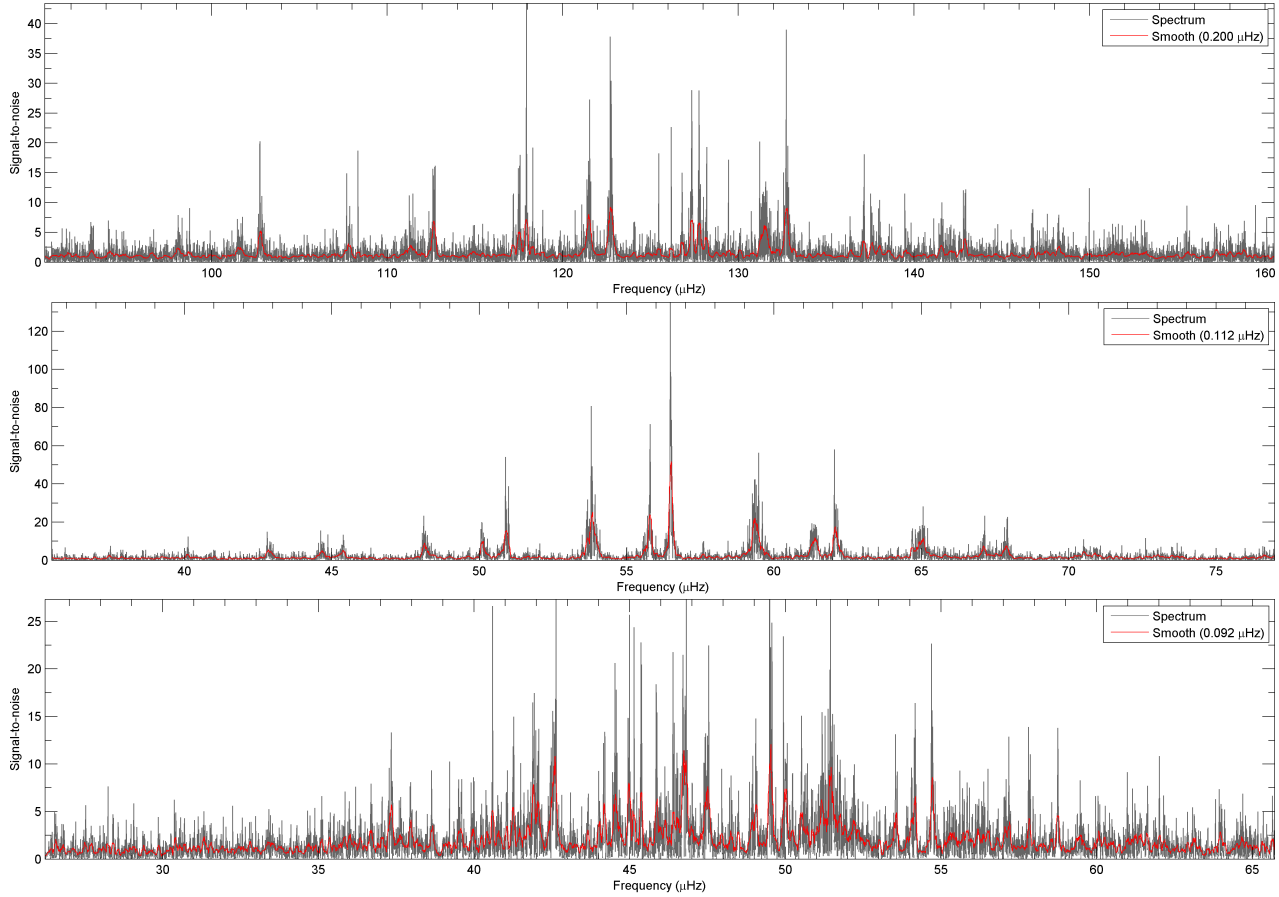
Fig. 1 Examples of the different empirical classes of giant stars in NCG 6819. Spectra have been divided with the fitted background so are here presented in units of signal-to-noise. *Top panel*: Low RGB star. *Middle panel*: High RGB star with clean dipole spectra. *Bottom panel*: Red clump star with complicated oscillation spectrum.

the (average) dipole modes for the high RGB stars, and the individual mixed modes for the low RGB stars.

5 Average seismic parameters and fundamental stellar properties

From the fitted radial mode frequencies we are able to construct $\Delta\nu$ and ϵ (Eq. 1). This is done by a weighted linear fit to the observed radial mode frequencies as a function of radial order, n. The same procedure can easily be applied to theoretical model frequencies as well, allowing for direct comparison. This fact should not be underestimated since usually $\Delta\nu$ is measured by means of the autocorrelation or power spectrum of the power spectrum, and hence can not be directly compared with the $\Delta\nu$ constructed from model frequencies.

In Kallinger et al. (2012) it was reported that the ϵ parameter could be used to distinguish the evolutionary state between RGB and RC when calculated from the three central radial modes. In this work we do not find that distinction, neither when using only the central three modes or when using all available radial modes. Especially when taking into account the formal errorbars on ϵ a distinction be-

tween RBG and RC is very difficult. Whether this is an effect of the particular chemical composition or mass of this cluster has not yet been determined. However, we do find that the small frequency separation, $\delta\nu_{02}$, does an excellent job of distinguishing between RGB and RC stars, as it is shown in Fig. 2. See e.g. Montalbán et al. (2010a,b, 2012) for extensive theoretical studies of $\delta\nu_{02}$. We also verified using stellar models that there indeed is a separation in $\delta\nu_{02}$ between the RGB and RC stars (see lower panel of figure 2). The separation is mass-dependent and reproduces the measurements for a mass around $1.6\,M_\odot$. From the models it seems that this is indeed a good indicator of evolutionary state, without having to measure the often difficult period-spacings, ΔP. However, for less massive stars ($\sim 1.1\,M_\odot$) the separation is less pronounced and will likely be less clear and within the error of the measurements. As an example, Corsaro et al. (2012) saw no clear separation for the open cluster NGC 6791, but an enlarged scatter around the position of the RC.

When $\Delta\nu$ and $\nu_{\max}$ have been measured, masses and radii of the stars can be determined using *scaling relations*
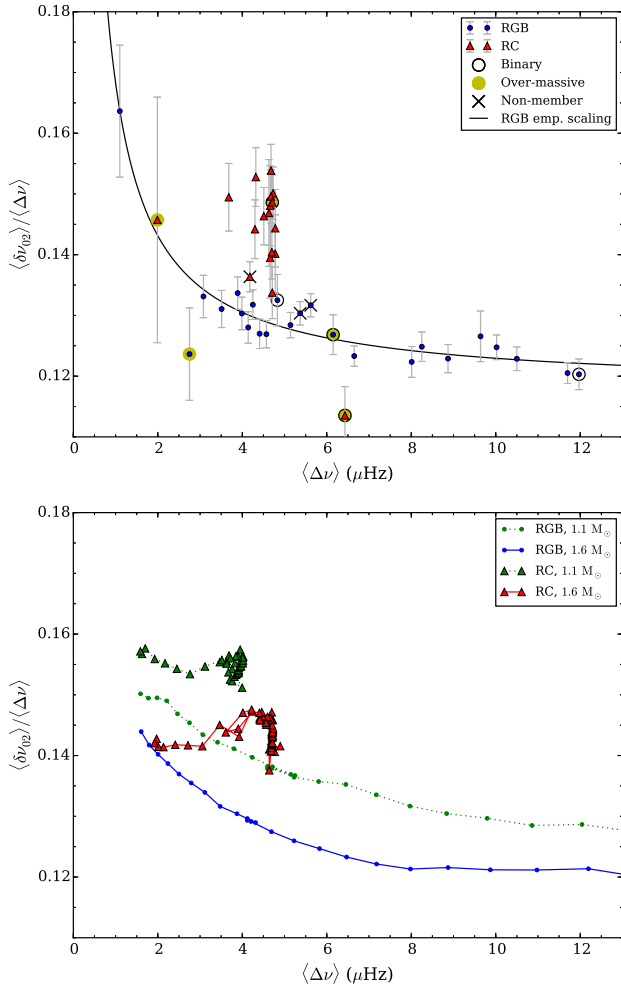
Fig. 2 *Top panel*: Measurements of average $\delta\nu_{02}/\Delta\nu$ for the cluster stars. Blue points indicate RGB stars, red points indicate RC stars. The solid line indicates a linear fit of $\delta\nu_{02}$ vs. $\Delta\nu$ of the RGB stars, excluding non-members and over-massive stars. *Lower panel*: Stellar model tracks showing the same thing, for two different masses. As can be seen the RGB and RC stars separate out.

(Brown et al. 1991; Kjeldsen & Bedding 1995):

$$\frac{R}{R_\odot} = \left(\frac{\Delta\nu}{\Delta\nu_\odot}\right)^{-2}\left(\frac{\nu_{max}}{\nu_{max,\odot}}\right)\left(\frac{T_{eff}}{T_{eff,\odot}}\right)^{1/2} \tag{7}$$

$$\frac{M}{M_\odot} = \left(\frac{\Delta\nu}{\Delta\nu_\odot}\right)^{-4}\left(\frac{\nu_{max}}{\nu_{max,\odot}}\right)^3\left(\frac{T_{eff}}{T_{eff,\odot}}\right)^{3/2}. \tag{8}$$

But in the case of star clusters where we can obtain the distance from independent methods, and hence the luminosity of the stars L, the mass-relation can also be written as (Miglio et al. 2012):

$$\frac{M}{M_\odot} = \left(\frac{\Delta\nu}{\Delta\nu_\odot}\right)^{12/5}\left(\frac{\nu_{max}}{\nu_{max,\odot}}\right)^{-14/5}\left(\frac{L}{L_\odot}\right)^{3/10} \tag{9}$$

We are therefore able to test scaling relations both to the cases where the distance is known, but also to values obtained by detailed stellar modelling.

6 Detection of Helium II ionization zone

Having obtained individual oscillation frequencies allows us to obtain more detailed information about the stellar structure in addition to to the fundamental stellar properties. One example of this is *acoustic glitches* which are signals imprinted in the individual oscillation frequencies caused by an abrupt change in the sound-speed somewhere in the star. For red giant stars, the main contributor to acoustic glitches is the helium II ionization zone. The imprint on the oscillation frequencies is an oscillation in difference between frequencies, which is emphasized by constructing the second differences between frequencies (Broomhall et al. 2014; Houdek & Gough 2007):

$$\Delta_2\omega_{n\ell} = A\omega_{n\ell}\exp(-2b^2\omega_{n\ell}^2)\cos(2\tau\omega_{n\ell} + 2d) + k, \tag{10}$$

where $\omega_{n\ell}$ is the angular version of $\nu_{n\ell}$, τ is the acoustic depth of the helium II ionization zone, A is the amplitude of the signal, b is a damping factor, d is a phase shift and k is a constant.

The detection of acoustic glitches in red giant stars are often hindered by the limited number of modes available, since constructing the second differences effectively removes points to be fitted and since all $\ell > 0$ modes are all potentially influenced by mixed modes, they can not be used directly.

By including the weighted averages, or nominal p-mode frequencies, of the dipole and quadrupole modes, as mentioned previously mentioned, we are able to provide much better constraints on a fit to Eq. (10), because particularly the dipole modes fills the gaps between the radial modes, resulting in much better coverage of the frequency axis.

Work is still ongoing to perform these fits on all the cluster stars, and the hope is that it may be possible to put constraints on the helium content of the cluster, by combining the individual measurements from all the stars.

7 The future of cluster asteroseismology

From this ongoing study of the open cluster NGC 6819 the conclusion is that clusters where asteroseismic studies are possible offer an absolute treasure chest of information – but what does the future hold for cluster asteroseismology?

Several missions, past, present and future, like CoRoT (Baglin et al. 2006), *Kepler*, K2, TESS (Ricker et al. 2014) and PLATO (Rauer et al. 2014), will do asteroseismology as part of their scientific program. However, asteroseismic studies in clusters are a different story.

In Fig. 3 a mosaic of the *Kepler* observations of NGC 6819 is shown. As it can be seen, near the centre of the cluster, the relatively large pixel-size of the Kepler instrument (4″-by-4″) means that observed targets overlap significantly and can not be separated from each other. With *Kepler*s successor, K2, the same problem is of course true, but furthermore complicated by the constant movement due
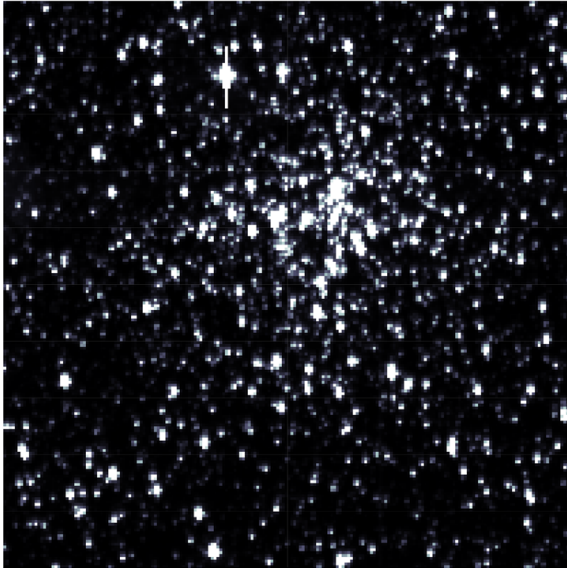
Fig. 3 The open cluster NGC 6819 as seen by *Kepler*. Note the many overlapping targets near the cluster centre even in this relatively uncrowded open cluster. The pixel-scale here is 3.98″.

Mission	Typical time span	Pixel size
CoRoT	120 days	2.32″
Kepler	4.5 years	3.98″
K2	75 days	3.98″
TESS	27 days	21″
PLATO	1 year?	15″

Table 1 Comparison of key characteristics of past, present and future photometric space-missions doing asteroseismology.

to the unstable spacecraft pointing, which smears out the point-spread-function of the instrument. And where *Kepler* was able to offer a very long timespan of near-continuous observations, K2 will only offer a small fraction of this, in the end yielding a much lower frequency resolution in the measured power spectra as well as a higher noise-level. It is possible to do limited studies of clusters using K2 (see eg. Miglio et.al. in preparation), but the number of targets will be limited and it will be unlikely to obtain asteroseismic information beyond the global asteroseismic parameters. For the upcoming missions TESS and PLATO the problem of crowding will be even more significant as these missions have even larger pixel-sizes (see Table 1). In these cases the central regions of open clusters and particularly globular clusters will be severely contaminated.

Another complication comes from the fact that the next generation of asteroseimic missions are focusing on bright stars. There are obvious reasons to do this, since it will give a much better signal-to-noise for asteroseismic signals, and are much easier for follow-up observations, like for instance spectroscopy or interferometry. However, this effectively rules out asteroseismic studies of most clusters, since these are in general much fainter than the detection limits of these missions.

In table 1 the characteristics mentioned above are listed for the past, present, and upcoming space-missions, that will do asteroseismology.

8 Conclusions

As previously mentioned, the asteroseismic study of the open cluster NGC 6819 is a veritable treasure chest of in-formation which will provide unique and strong constraints on stellar structure and evolution. This is both due to the unique sample of stars in the cluster, sharing common chemical composition, distance and age, but also because of the long uninterrupted measurements from the *Kepler* mission which allows us to perform these detailed studies. In this work we have reported on how we are now able to perform detailed peakbagging of the red giant stars in open clusters and use these measurements in various ways to constrain stellar models and hence our understanding of stellar structure and evolution.

The unfortunate conclusions that is drawn from a look at the various space missions aiming to do asteroseismology in the future, is that we are unlikely to see any better data for cluster asteroseismology than what *Kepler* has already provided us. It seems that no upcoming mission is going to yield a comparable time-coverage or spatial resolving power to make them useful for these kind of analyses. The pressing question is then: do we need to do something about this? Should we consider a space-based mission dedicated to cluster asteroseismology?

References

Baglin, A., Michel, E., & Auvergne, M. 2006, in SOHO 18/GONG 2006/HELAS I, Beyond spherical Sun, ed. Michael Thompson, Vol. 624 (Sheffield, UK: ESA Special Publication), 34

Basu, S., Broomhall, A.-M., Chaplin, W. J., & Elsworth, Y. 2012, Astrophys. J., 758, 43

Bedding, T. R., Mosser, B., Huber, D., et al. 2011, Nature, 471, 608

Borucki, W. J., Koch, D., Basri, G., et al. 2010, Science (80-.)., 327, 977

Broomhall, a.-M., Miglio, A., Montalban, J., et al. 2014, Mon. Not. R. Astron. Soc., 440, 1828

Brown, T. M., Gilliland, R. L., Noyes, R. W., & Ramsey, L. W. 1991, Astrophys. J., 368, 599

Chaplin, W. J., Basu, S., Huber, D., et al. 2014, Astrophys. J. Suppl. Ser., 210, 1

Corsaro, E., Stello, D., Huber, D., et al. 2012, Astrophys. J., 757, 190

Handberg, R. & Campante, T. L. 2011, Astron. Astrophys., 527, A56

Handberg, R. & Lund, M. N. 2014, Mon. Not. R. Astron. Soc., 445, 2698

Harvey, J. 1985, in ESA Futur. Mission. Solar, Heliospheric Sp. Plasma Phys., ed. E. Rolfe & B. Battrick, 199–208

Houdek, G. & Gough, D. O. 2007, Mon. Not. R. Astron. Soc., 375, 861

Kallinger, T., Hekker, S., Mosser, B., et al. 2012, Astron. Astro-phys., 541, A51

Kallinger, T., Mosser, B., Hekker, S., et al. 2010, Astron. Astro-phys., 522, A1

Karoff, C. 2008, PhD thesis, Aarhus University

Kjeldsen, H. & Bedding, T. R. 1995, Astron. Astrophys., 293, 87

Miglio, a., Brogaard, K., Stello, D., et al. 2012, Mon. Not. R. As-tron. Soc., 419, 2077

Montalbán, J., Miglio, A., Noels, A., Scuflaire, R., & Ventura, P. 2010a, Astron. Nachrichten, 331, 1010

Montalbán, J., Miglio, A., Noels, A., Scuflaire, R., & Ventura, P. 2010b, Astrophys. J., 721, L182

Montalbán, J., Miglio, A., Noels, A., et al. 2012, Astrophys. Sp. Sci. Proc., 26, 23

Mosser, B., Belkacem, K., Goupil, M. J., et al. 2011, Astron. As-trophys., 525, L9

Mosser, B., Goupil, M. J., Belkacem, K., et al. 2012, Astron. As-trophys., 540, A143

Quirion, P. O., Christensen-Dalsgaard, J., & Arentoft, T. 2010, As-trophys. J., 725, 2176

Rauer, H., Catala, C., Aerts, C., et al. 2014, Exp. Astron., 38, 249

Ricker, G. R., Winn, J. N., Vanderspek, R., et al. 2014, J. Astron. Telesc. Instruments, Syst., 1, 014003

Silva Aguirre, V., Davies, G. R., Basu, S., et al. 2015, Mon. Not. R. Astron. Soc., 452, 2127